Electronic Supplementary Information (ESI)

Hierarchically order porous Lotus shaped nano-structured MnO_2 through $MnCO_3$: Chelation Mediated growth and shape dependent improved catalytic activity

*Provas Pal, Sandip Pahari, Arnab Kanti Giri, Sagar Pal, Hari C. Bajaj, Asit Baran Panda **

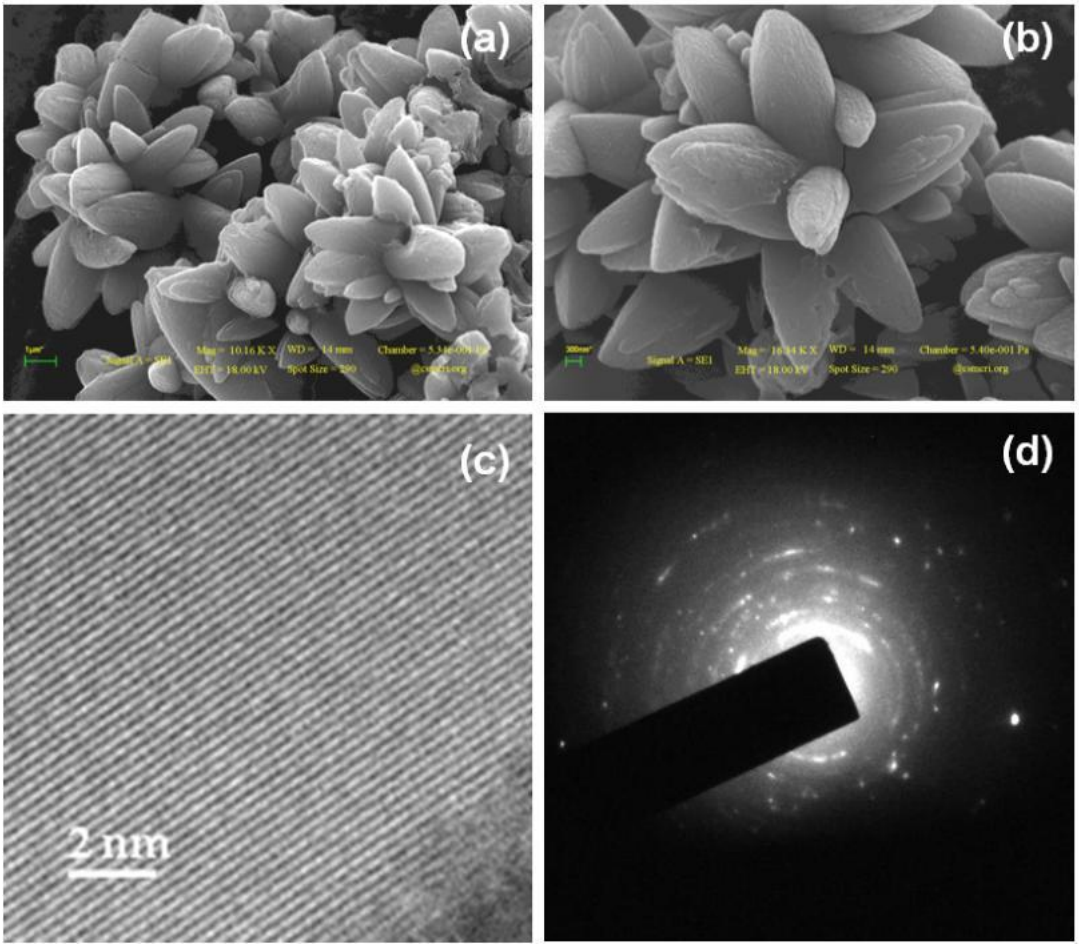

Fig. S1. SEM (a, b), HR-TEM (c) images and electron diffraction pattern (d) of lotus shaped MnO_2 calcined at 350 °C/6h.

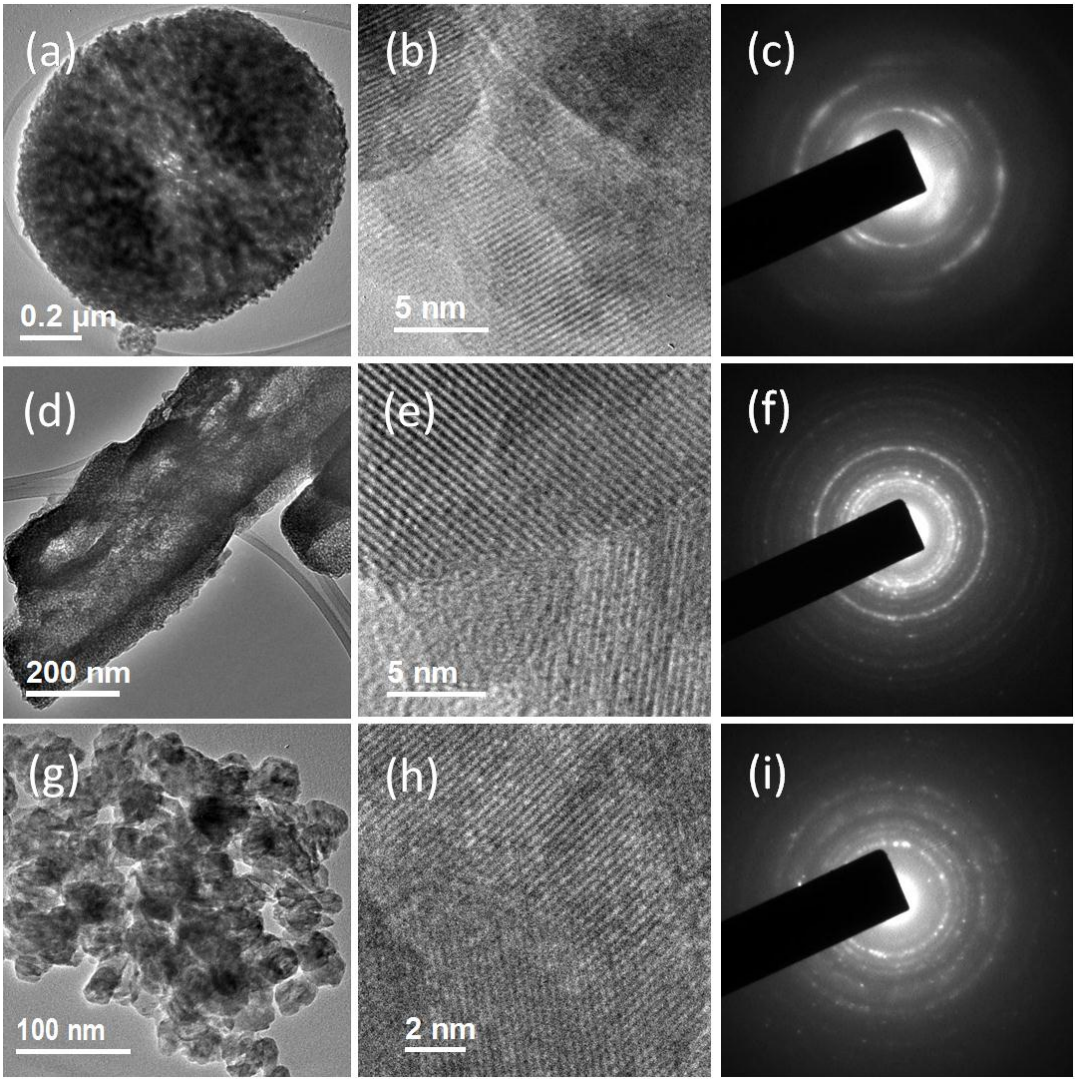

Fig. S2. TEM, HR-TEM images and electron diffraction patterns of Sphere (a, b, c), rod (d, e, f) and agglomerated (g, h, i) MnO_2 particles synthesized in presence of oxalic acid, tartaric acid and EDTA, respectively, followed by calcination at 350 °C/6h.

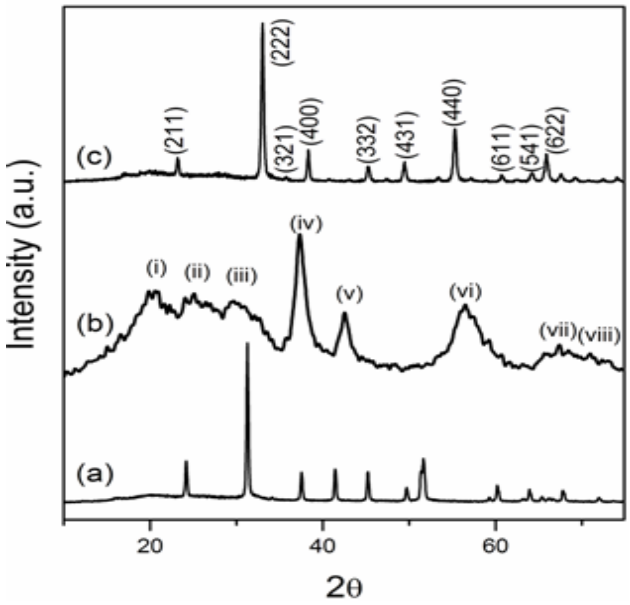

Fig. S3. X-ray diffraction of parental lotus shaped (a) $MnCO_3$, (b) γ-MnO_2 and (c) Mn_2O_3 calcine at 600 C/6h.

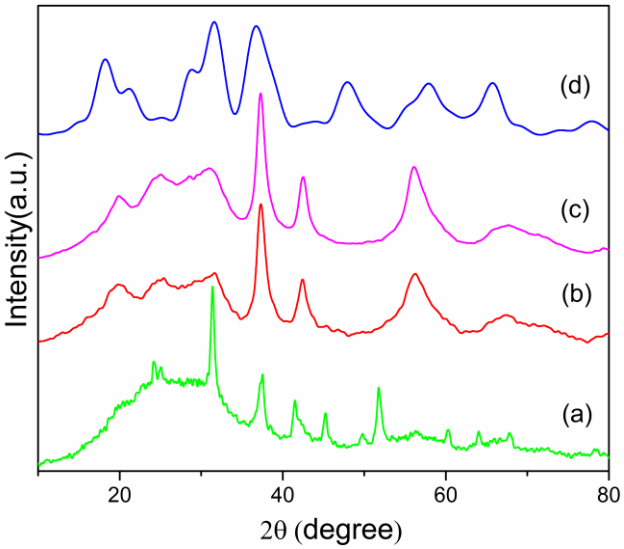

Fig. S4. X-ray diffraction of (a) agglomerated, (b) Lotus, (c) Spherical and (d) Rod shaped MnO_2.

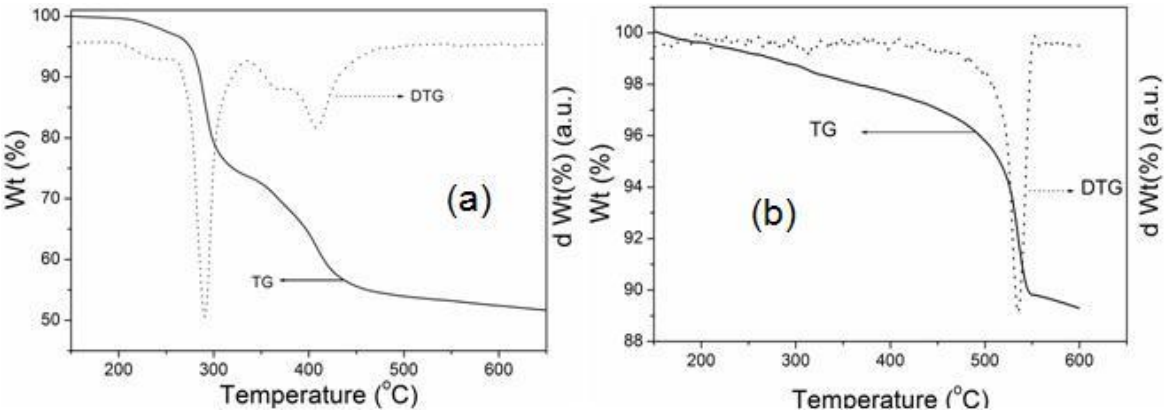

Fig. S5. TG curves of perental lotus shaped $MnCO_3$ as well as the MnO_2 calcined at 350°C for 6h.

Thermo-gravimetric analysis was performed, to understand the exact thermal effect on the as-synthesized $MnCO_3$. From the TGA and DTG curve of the as-synthesized $MnCO_3$ in air, it is evident that initially the weight loss of ~4-5% in the temperature range of 50 -220 °C can be attributed to the removel of adsorbed water molecule, trapped carbon dioxide, and ammonia from the $MnCO_3$ moiety. In the 2nd step the major weight loss ~ 30 % in the temperature range of 220-350°C can be assigned to the loss of CO_2 due to the transformation of $MnCO_3$ to tetravalent Mn^{4+} oxide (MnO_2). [1] The theoretical weight loss value for the transformation of $MnCO_3$ to MnO_2 is 24.34%. The excess weight loss is probably originating from the decomposition of strongly adsorbed citric acid, present even after through washing. Further ~ 15% weight loss observed above 350 °C (350-500 ° C) can be attributed to the reduction of tetravalent Mn^{4+} oxide (MnO_2) to Mn_2O_3 (9%) and decomposition of trapped citric acid. However, this unrecompensed citric acid remained even after 350°C during continuous heating in TG analysis was fully decomposed even in 350°C on long time (6h) calcinations. This was confirmed by the TG analysis of MnO_2 calcined at 350°C for 6h step-wise. During TGA of MnO_2, total 11% weight loss was observed. In the 11 %, theoretical 9% weight loss is for (MnO_2) to Mn_2O_3 transformation and 2% may be for the moisture within 250°C. This experiment confirmed that the synthesized MnO_2 is carbon free.

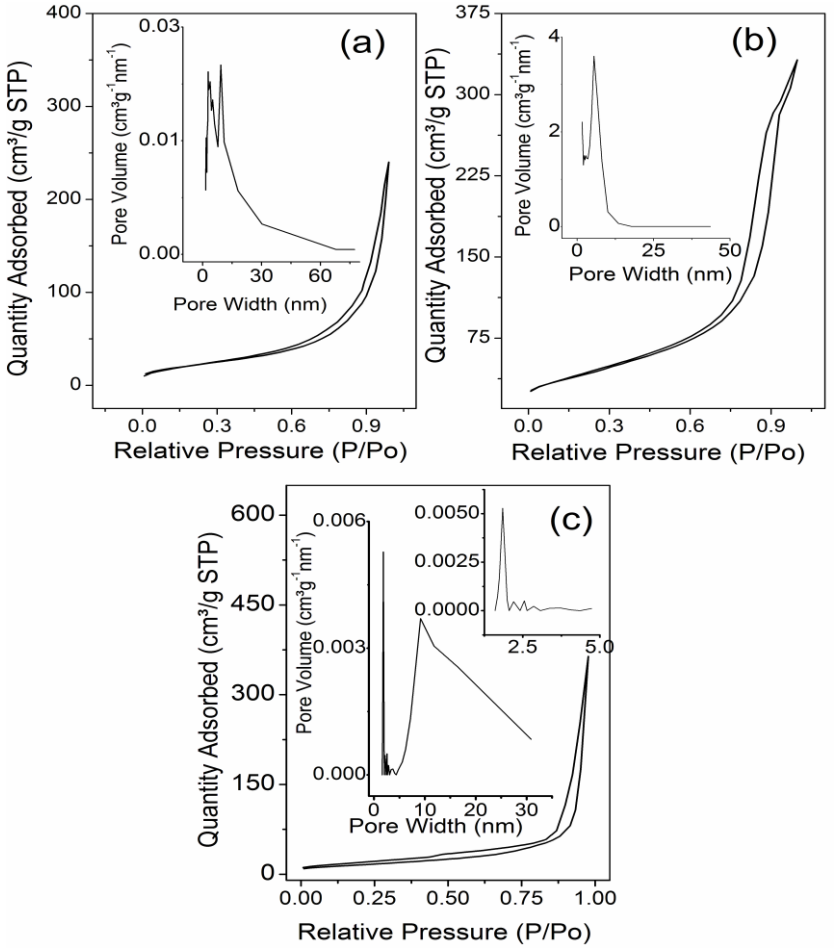

Fig. S6. BET Surface Area and pore size distribution curve (inset) rod (a), Sphere (b) and agglomerated (c) MnO_2 particles synthesized in presence of oxalic acid, tartaric acid and EDTA, respectively, followed by calcination at 350 °C/6h of synthesized MnO_2 of diierent shapes, Mn_2O_3

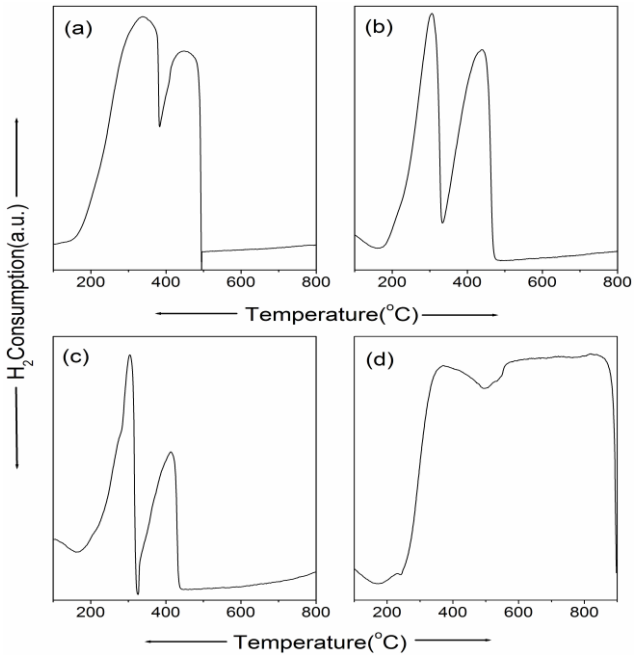

Fig. S7. H_2-TPR curve of Sphere (a), rod (b) and agglomerated (c) MnO_2 particles synthesized in presence of oxalic acid, tartaric acid and EDTA, respectively, followed by calcination at 350 °C/6h and commercially available bulk MnO_2 (d).

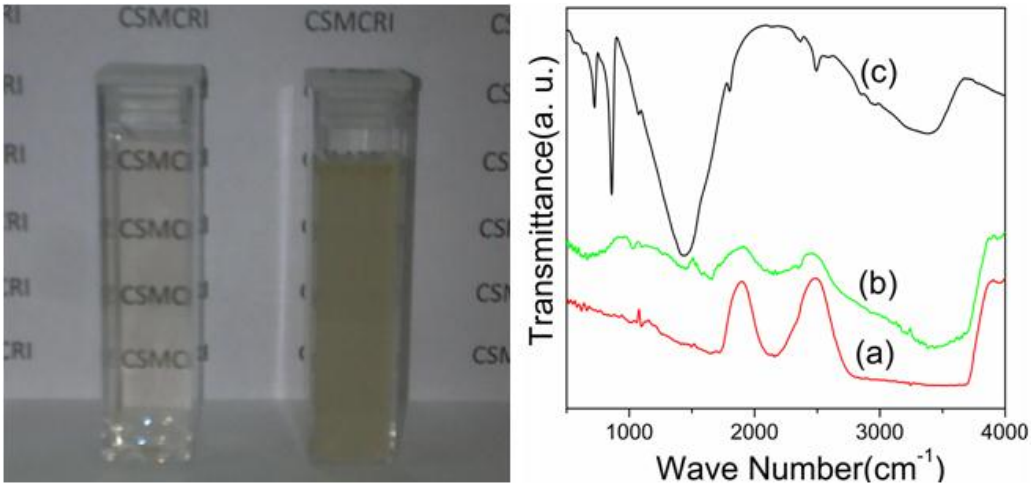

Fig. S8. Left column: The photograph of initial clear precursor solution and hazy solution after 1 h. right colume: Solution phase IR for detection of formation of $MnCO_3$ Caped by citrate ion (a) clear solution, hazy solution (after 1h) and pure $MnCO_3$ formed without chelating agent.

Though in solution phase structure and stoichiometry determination is really tuff but 3 CA are coordinated to $MnCO_3$ and is capped nucleated MnCO3 Nano blocks by carboxyl groups in different orientation. This interaction of CAs and $MnCO_3$ Blocks has been proven by FT-IR study. The peak of hydroxyl groups of nano-$MnCO_3$ down shifts in clear solution of $MnCO_3$-Citrate Solution and after 1h when some $MnCO_3$ precipitate then two peaks has observe one more down shifted and another at higher region due to low concentrated with higher binding strength of hydroxyl group of nano-$MnCO_3$ and pure hydroxyl group respectively. Also the band at 1725 cm^{-1} shifted to 1665 cm^{-1} probably is caused by ν(C=O) that is shifted by intermolecular hydrogen bonds to lower wave number when after 1h some $MnCO_3$ precipitated out. Also a comparison of this spectrum with that of the citrate adsorbed on nano-$MnCO_3$ revealed a widening and a shift to higher frequencies of ν (COO^-) at 1574 cm^{-1} for the clear solution of $MnCO_3$-Citrate solution.
Lastly a broad peak at 1430 cm^{-1} indicates for ν (C-0) of $MnCO_3$. Which are presents both the spectra of $MnCO_3$-Citrate solution (clear and hazy).

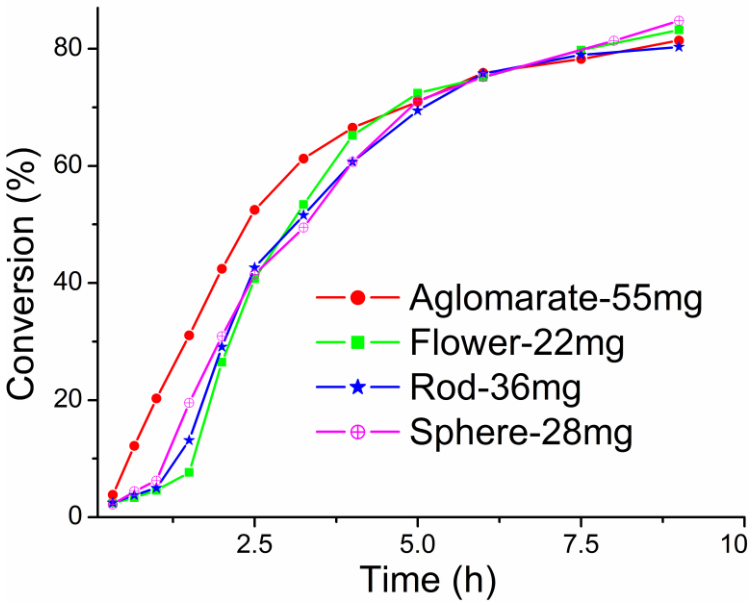

Fig. S9. Reaction profiles of α-pinene oxidation using molecular oxygen of four different shapes catalysts keeping constant S_{BET} and at other condition. All the data points are within the error range of ±2.

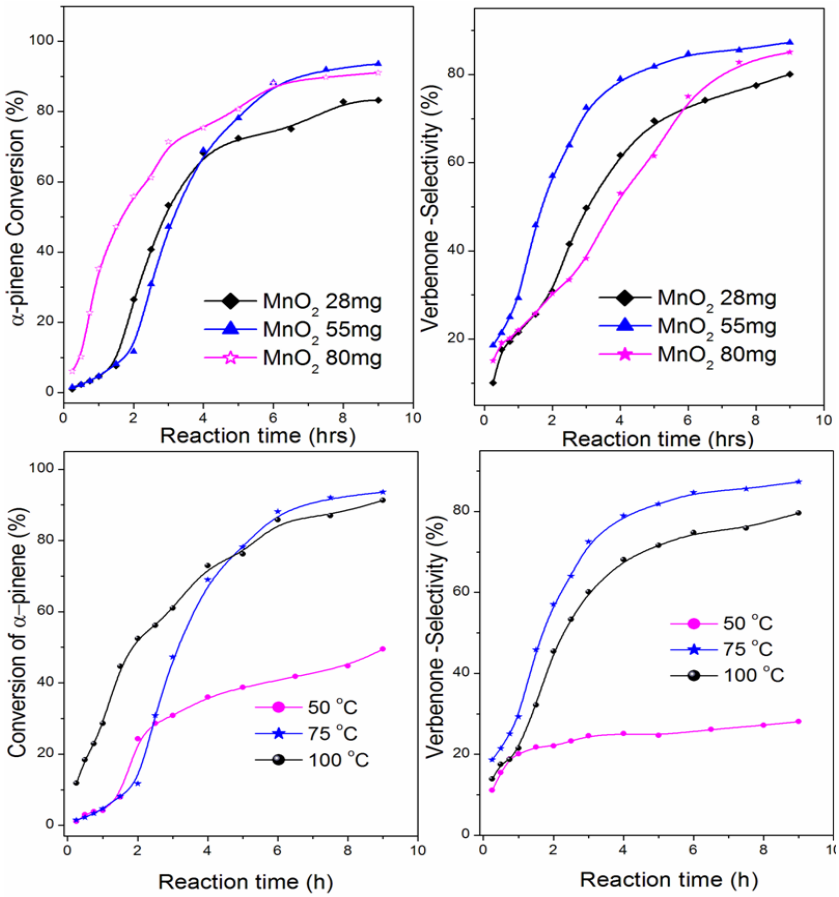

Fig. S10. Reaction profiles of α-pinene oxidation using lotus shaped MnO_2 as catalyst and molecular oxygen in 35.2 mmol α -Pinene (4 ml) with varying amount of catalyst and reaction temperature. All the data points are within the error range of ±3.

It was observed that 55 mg of catalyst for 4 ml α - Pinene and 75 °C is the optimized reaction condition with respect to conversion and selectivity and in the optimized reaction conditions. Maximum 94% conversion of α-pinene with 87% selectivity of verbenone was observed. The conversion was decreased with reduced amount of catalyst, in the same time the selectivity of verbenone was also decreased with enhanced verbenol selectivity. With further increase in the catalyst amount, initial reaction rate was increased reasonably but after 8h the conversion was almost same as reaction performed with optimized amount of catalyst. Likewise, at lower temperature, the conversion as well as selectivity of verbenone was very less, whereas at higher temperature the initial reaction rate was high but after 8 h maximum conversion was observed in short period (similar to high catalyst loading). However, high temperature affects the selectivity of verbenone and it decreased at higher temperature.

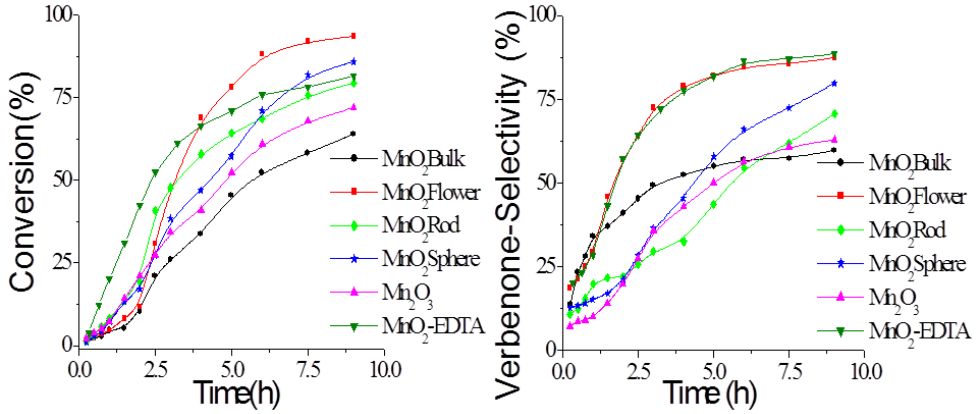

Fig. S11. Reaction profiles of α-pinene oxidation using molecular oxygen in 35.2 mmol α -Pinene (4 ml), 55 mg catalyst with varying shapes and at 75 °C. All the data points are within the error range of ±3.

The catalyst showed a similar profile with more than 60% α-pinene conversion. All the performed reaction ended with 6 probable compounds with varying selectivity. However, all the catalyst resulted >50% selectivity of verbenone. The synthesized lotus shaped MnO_2 showed much superior catalytic activity than that of bulk MnO_2, with respect to conversion as well as selectivity of verbenone. Further, the conversion and selectivity of lotus shaped MnO_2 was better than that of MnO_2 spheres as well lotus shaped Mn_2O_3. Lotus shaped MnO_2 showed superior activity most probably due to it high surface area as well as much more accessible surface reactant originating from its shape, and presence of more low temperature labile oxygen species.

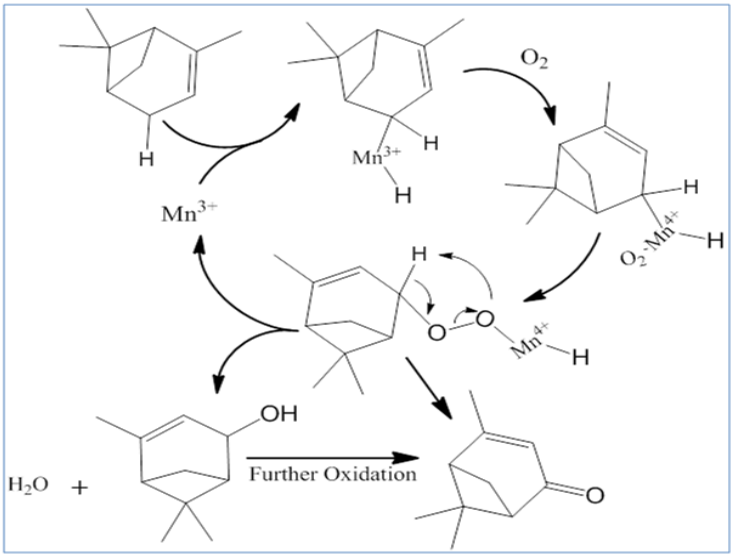

Scheme S1 Proposed probable reaction mechanism.

Manganese oxide structures can form mixed-valent octahedral molecular sieves. Suib et. al describe that the active sites of OMS may be derived from Mn^{3+} ions in tunnel sites in the materials.[3]. The form of active oxygen is presumably the O^{2-} ion; this indicates a

simultaneous transfer of two electrons and not a stepwise electron donation. This prediction also supports our results that oxidation reaction proceeds in presence of radical trapper. [4.]

Table S1. Catalytic activity comparison of the synthesized lotus shaped MnO_2 with other reported catalysts for oxidation of α-pinene.

Sr. No	Catalyst	Oxidant	Conversion (%)	Major products	Selectivity (%)	Yields (%) [a]	Ref. [b]
1	**MnO_2-lotus**	**O_2**	**94**	**Verbenone**	**87**	**81**	***Present work***
2	$Co(OAc)_2$	O_2	80	Verbenyl acetate	29.5	23	5
3	CuI	TBHP(Air)	98	Verbenone	36	35	6
4	$CoCl_2$,	O_2	84	Verbenone	39	32	7
5	Co^{2+}-zeolite	O_2	47	Epoxide	61	28	8
6	Ti-HMS	TBHP	30	campholenic aldehyde	80	24	9
7	Ru/Co-zeolite	Peroxide	75	Epoxide	35	26	10
8	NaOH	O_2	45	Verbenol	47	21	11
9	Cr-AlPO-5	TBHP	85	Verbenone	77	65	12
10	Cytochrome P450cam	O_2	70	Verbenone	86	60	13
11	Co^{3+}cubane-mSiO_2	O_2	81.5	Epoxide	50.1	40	14
12	$Cr(CO)_6$	TBHP	98	Verbenone	68	66	15
13	Co_3O_4	O_2	76	Epoxide	84	63	16

[a] The mentioned yields are theoriticla yields calculated from conversion and selectivity; [b] all the catalytic results of respective catalysts mentioned from Sr. No. 2-13 are literature reported results.

Catalyst used in Sr no. 2,3,4,8,12 are homogeneous and rest are heterogeneous. In the used heterogeneous catalysts only Cr-AlPO-5 (Sr. No 9) resulted both the conversion and selectivity of >80%. Still its theoritical yield is much less (65%) than that of synthesized lotus shaped MnO_2 (81%). Moreover, use of toxic Cr in catalyst and TBHP as oxident makes the procedure non-viable.

Reference:

1 L. Wang, F. Tang, K. Ozawa, Z-G. Chen, A. Mukherj, Y. Zhu, J. Zou, H-M. Cheng and G. Q. Lu, *Angew. Chem. Int. Ed.* **2009**, *48*, 7048.

2 S. J. Gregg and K. S. W. Sing, Adsorption, Surface Area and Porosity; Academic Press: London, **1982**.

3 Y-C Son, V D. Makwana, A R. Howell and S L. Suib *Angew. Chem. Int. Ed.* 2001, **40**, 4280.

4 D. Shevela, S. Koroidov, M. M. Najafpour, J. Messinger and P. Kurz, *Chem. Euro. J.* **2011**, *17*, 5415.

5 M. d. F. T. Gomes and O. A. C. Antunes, *J. Mol Catal A: Chem*. **1997**,*121*, 145.

6 B. A. Allal, L. E. Firdoussi, S. Allaoud, A. Karim,Y. Castanet and A. Mortreux, *J. Mol Catal A: Chem*. **2003**, *200*, 177.

7 M. K. Lajunen, M. Myllykoski and J. Asikkala, *J. Mol Catal A: Chem*. **2003**, *198*, 223.

8 M. V. Patil, M. K. Yadav and R. V. Jasra, *J. Mol Catal A: Chem*. **2007**, *277*, 72.

9 Y.-W. Suh, N.-K. Kim, W.-S. Ahn and H-K. Rhee, *J. Mol Catal A: Chem*. **2003**, *198*, 309.

10 T. Joseph, D. P. Sawant, C.S. Gopinath and S.B. Halligudi, *J. Mol Catal A: Chem*. **2002**, *184*, 289.

11 J. M. Encinar,F. J. Beltrán and J. M. Frades, *J Chem Tech Biotechnol*. **1994**, *61*, 359.

12 H. E. B. Lempers and R. A. Sheldon, *Appl. Cata. A: Gen* **1996,** *143*, 137.

13 S. G. Bell, X. Chen, R. J. Sowden, F. Xu, J. N. Williams, L.-L. Wong and Z. Rao, *J. Am. Chem. Soc*. **2003**, *125*, 705.

14 R. Chakrabarty, B. K. Das and J. H. Clark, *Green Chem.*, **2007**, *9*, 845.

15 Z. Yoosuf-Aly, J. A. Faraldos, D. J. Miller and R. K. Allemann, *Chem. Commun*., **2012**, *48*, 7040.

16 X.-H. Lu, Q.-H. Xia, D. Zhou, S.-Y. Fang, A.-L. Chen and Y.-L. Dong, *Catal. Commun.*, **2009**, *11*, 106.